J Math Chem (2009) 45:354–363
DOI 10.1007/s10910-008-9410-7

ORIGINAL PAPER

Retro–Leapfrog and structure elucidation

Mircea V. Diudea

Published online: 5 August 2008

Abstract Operations on maps are topological-geometrical tools used for transforming a given polyhedral tessellation. Investigation of fullerene structure often needs information on the original map which transformed into a larger molecular structure. Operations leading to the previous, smaller structures are called Retro-operations. They appear particularly useful in studies of structure elucidation or stability of series of fullerenes. The paper presents the first structure affiliation of the well-known C_{60} fullerene to a family of Leapfrog fullerenes with relatedness being established by map operation. Thus, the tessellation of C_{60} is described as an Archimedean, joint Sumanene-hexagon covering, in tetrahedral disposition. The other members of family show essentially the same covering and predicted good stability. Related Leapfrog fullerenes showing a disjoint Sumanene covering are also given.

Keywords Map operations · Retro-operations · Structure elucidation · Tessellation · Fullerenes

1 Introduction

A map M is a combinatorial representation of a surface [1]. Operations on maps are topological-geometrical transformations enabling modification of a polyhedral tessellation. Several operations on maps are known and used for various purposes, mainly for generating and modifying fullerene structure.

A classical fullerene is defined as a sphere-like molecule, consisting entirely of carbon atoms and being tessellated by 12 pentagons and a various number of hexagons ($v/2 - 10$). Non-classical fullerene extensions may include rings of other size [2–4].

M. V. Diudea (✉)
Faculty of Chemistry and Chemical Engineering, Babes-Bolyai University, 400028 Cluj, Romania
e-mail: diudea@gmail.com

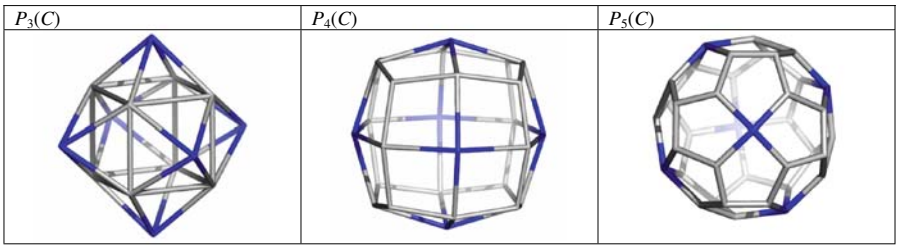

Fig. 1 P_r *capping*($r = 3,4,5$) applied to the cube C; for other operation names the reader may consult www.georgehart.com/virtual-polyhedra/conway_notation.html

Basic map operations, such as dualization *Du*, truncation, *Tr* stellation *St*, medial *Me*, etc., are well-known and have been described elsewhere [4–6]. Recall some basic relations in a map [7]:

$$\sum d v_d = 2e \tag{1}$$

$$\sum s f_s = 2e \tag{2}$$

where v is the number of vertices, e the number of edges, f the number of faces, d the vertex degree, v_d the number of vertices of degree d and f_s the number of s-gonal faces. These two relations are combined in the Euler formula [8]:

$$v - e + f = 2(1 - g) \tag{3}$$

In (3), g is the *genus* [9] of a map embedded in a given surface; it counts the holes to be performed in the sphere to make it homeomorphic to the considered surface. In case of sphere, $g = 0$, while for the torus $g = 1$. An *embedding* is a drawing of a graph on a surface with no crossing lines.

An extension of stellation, called p*olygonal* P_r *capping* ($r = 3, 4, 5$), was yet published [10]. A P_r capping is achieved as: add a new vertex in the center of the face. Put $r - 3$ points on the boundary edges. Connect the central point with one vertex (the end points included) on each edge. In this way the parent face is covered by trigons ($r = 3$), tetragons ($r = 4$) and pentagons ($r = 5$). P_3 operation is just the well-known *stellation* or (centered) *triangulation*. In case of a regular map, the transformed map shows the relations:

$$P_r(M): \quad v = v_0 + (r - 3)e_0 + f_0; \quad e = re_0; \quad f = s_0 f_0 \tag{4}$$

so that the Euler's relation holds. The subscript zero refers to the parent map, in our case the Platonic solids: tetrahedron T, Octahedron O, cube C, dodecahedron D and icosahedron I. Recall the dual-pairs: $T\&T$ (self-dual); $O\&C$ and $D\&I$. Figure 1 gives examples of the operations realization, starting from cube.

2 Leapfrog and Retro–Leapfrog

Leapfrog Le is a composite operation that can be written as [11–14]:

$$Le(M) = Du(P_3(M)) = Tr(Du(M)) \tag{5}$$

A sequence of stellation-dualization $P_3 - Du$ rotates the parent s-gonal faces by π/s. Leapfrog operation is illustrated, for a pentagonal face, in Fig. 2.

The map transformed parameters are:

$$Le(M): \quad v = s_0 f_0 = d_0 v_0; \quad e = 3e_0; \; f = v_0 + f_0 \tag{6}$$

A bounding polygon, of size $2d_0$, is formed around each original vertex. In the most frequent cases of 4- and 3-valent maps, the bounding polygon is an octagon and a hexagon, respectively (Fig. 3).

If the map is a d_0 regular graph, the following theorem holds [15,16]:

Theorem 1 *The multiplication factor $m = v/v_0$ of the number of vertices in $Le(M)$ is d_0 irrespective of the tessellation type.*

Demonstration follows from the observation that, for each vertex of M, d_0 new vertices result in $Le(M)$: $m = v/v_0 = d_0 v_0/v_0 = d_0$. Consequently, in trivalent maps, $Le(M)$ is the *tripling* operation. Note that the vertex degree in $Le(M)$ is *always* 3, as a consequence of the involved triangulation P_3. In other words, dual of a triangulation is a *cubic/trivalent net* [1]. It is also true that truncation always provides a trivalent net.

A classical example of using *Le* operation is: $Le(D) = C_{60}$ fullerene. The Leapfrog operation can be used to insulate the parent faces by surrounding polygons of $2d_0$ folding.

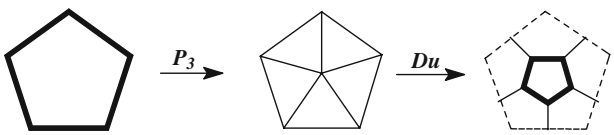

Fig. 2 The Leapfrog *Le* operation on a pentagonal face

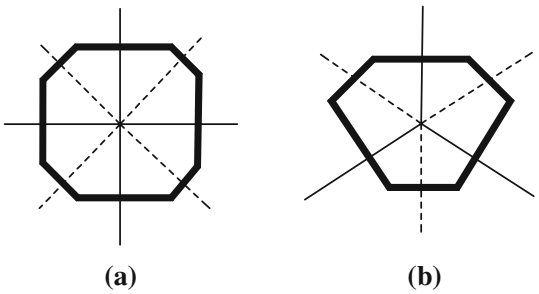

Fig. 3 Bounding polygons around a 4-degree (**a**) and 3-degree (**b**) vertex by*Le* operation

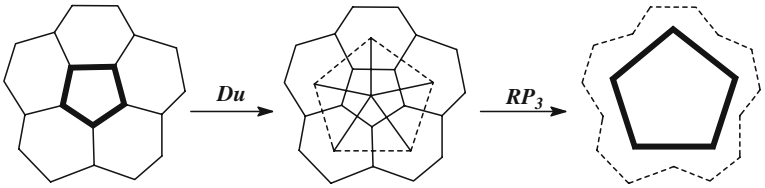

Fig. 4 The Retro–Leapfrog operation on a pentagonal face

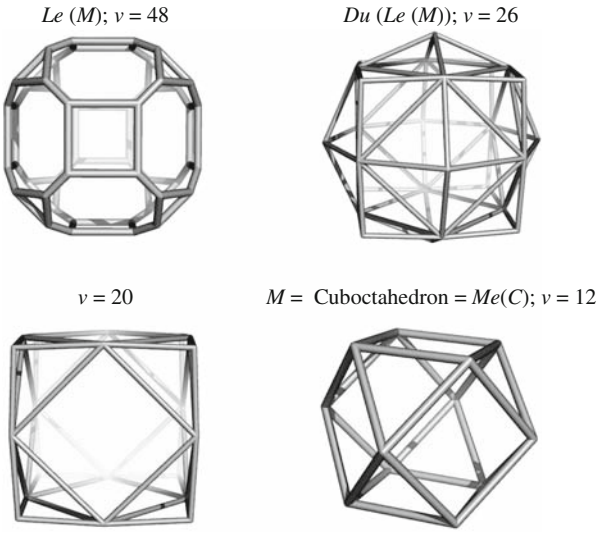

Fig. 5 The Retro–Leapfrog operation applied on a cage of 48 vertices

Retro–Leapfrog operation is based on the following sequence [17]:

$$RLe(M) = RP_3(Du(Le(M))) \tag{7}$$

It is performed by cutting off all the vertices of lowest degree in the dual (of Leapfrogged map—Fig. 4).

The Retro-operation is specified by the prefix "*R*". Recall that, dualization *Du* is achieved by putting a point in the centre of each face and joining those points whose faces share an edge; RP_3 in the above is the Retro-stellation. In a 3D representation, *RLe* is illustrated in Fig. 5.

3 Structure elucidation

There is no difficulty in recognizing the parent of a polyhedral structure having the number of atoms v divisible by 3. Problems appear in case of irregular maps, when the above theorem must be considered for each vertex, thus a non-integer *m*-value resulting.

(a) 240*C/O*-30= $Le(P_5(Me(C)))$ 240*C*-30RO=$RO(Tr_s(Ca_{3,2,C}(Me(C))))$ 6×[8:(5,6)$_4$]JFw & 8×[6:(5,6)$_3$]JFw & 12×JR_8	**(b)** $R(Le(P_5(Me(C)))) = P_5(Me(C))$ v=74; (12+6) × $v(d$=4)
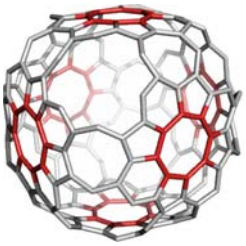	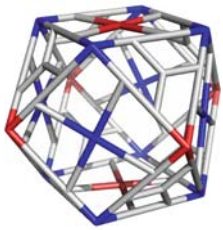

Fig. 6 A sumanene-covered cage and its Retro–Leapfrog *RLe* transform

(a) 240*C/O*-30= $Le(P_5(Me(C)))$ 240*C*-30RO=$SW(Tr_s(Ca_{3,2,C}(Me(C))))$ 8×[6:(5,6)$_3$]JFw & 6×[8:(5,6)$_4$]JFw & 12×JR_8	**(b)** 240*C/O*-30= $Le(P_5(Me(C)))$ 12×[8:(5,6)$_4$]JFw & 8×JR_6 & 6×JR_8
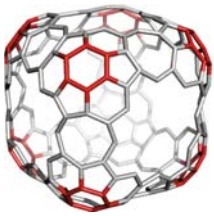	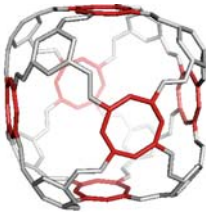

Fig. 7 Sumanenic covering

In case of cage $240C/O-30$ (Fig. 6a), *RLe* led to a cage having all faces pentagonal and vertices of degree 3 and 4. It appears to be a transform of P_5 operation, thus an RP_5 has to be performed as follows: join by an edge every two vertices of 4-degree located at the topological distance 3 (see the P_5 definition above) and delete all the 3-degree vertices. The resulting cage is the cuboctahedron, a medial transform of either dual-pair cube/octahedron, as can bee seen by looking at the 4-degree vertices located in the corners of Fig. 6b.

Resuming to the sequence of map operations generating $240C/O-30$RO (Fig. 6a), it can be written as: $Le(P_5(Me(M)))$ or simply as $Le(P_5(M))$, the medial being used to provide vertices of degree 4. The multiplication factor is $m = 10d_0$ in the triangulated Platonic or $m = 30$ in the trivalent dual pair, for the sequence involving the medial operation, and $m = 5d_0$ or $m = 15$ in case of the last, simplified sequence.

The covering of the cage $240C/O-30$RO can be described either by the sumanenic flower located in the centers of faces $6 \times$ [8:(5, 6)$_4$]JFw and corners $8 \times$ [6:(5, 6)$_3$]JFw (Figs. 6a and 7a) or by the sumanenic flowers located on the twelve edges of the cube $12 \times$ [8:(5, 6)$_4$]JFw (Fig. 7b). Sumanene is a real molecule, recently synthesized [18,19].

The same object can be obtained by SW edge-rotation from $240C/O-30$ (Fig. 8a), by rotating the spokes of the corazulenic flowers [4:(7(5c)$_4$]Fw. The tessellation of this

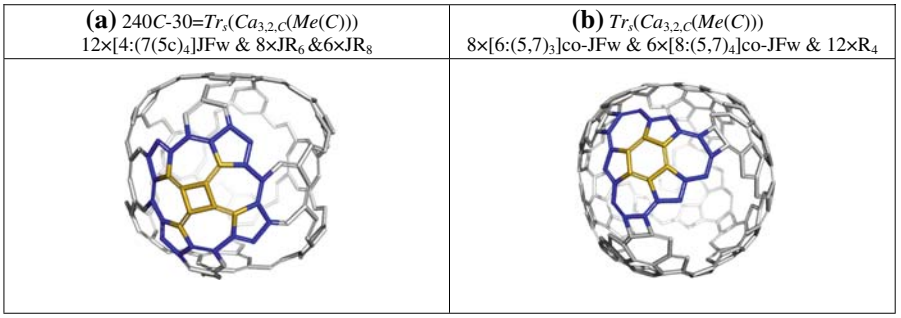

Fig. 8 Corazulene and corazene as Fw and co-Fw patterns

Table 1 Data for cages designed by $Le(P_5(M))/Le(P_5(Me(M)))$ operation sequences: heat of formation per atom, HF (kcal/mol); HOMO-LUMO Gap (eV); HF/Gap (×100; eV; PM3); strain energy per atom SE (kcal/mol; POAV1); total π-electron energy E_π (β-units; simple Hückel) and HOMA index of aromaticity

	Cage	Sym.	HF	Gap HF/Gap	SE	E_π shell	HOMA	HOMA-Fw	Fw
	1	**2**	**3**	**4**	**5**	**6**	**7**	**8**	**9**
1	$60T-15$	I_h	13.512	6.593	8.257	1.553	0.169	0.169	$4\times$ [6:(5, 6)$_3$]Fw
				8.893		cl		0.169	$4\times$ [6:(5, 6)$_3$]co-Fw
								0.375	$4\times$ JR$_6$
2	$120C/O-15$	O	12.454	6.015	4.566	1.543	−0.036	−0.054	$8\times$ [6:(5, 6)$_3$]JFw
	or $120T-30$			8.987		cl[a]		−0.688	$6\times$ JR$_8$
								0.116	$6\times$ [8:(5, 6)$_4$]co-JFw
								0.693	$8\times$ R$_6$
3	$240C/O-30$	O	10.666	5.530	3.002	1.537	0.068	0.177	$8\times$ [6:(5, 6)$_3$]JFw
				8.371		cl[a]		0.076	$6\times$ [8:(5, 6)$_4$]JFwf
								−0.123	$12\times$ JR$_{8e}$
								0.167	$12\times$ [8:(5, 6)$_4$]JFwe
								0.608	$8\times$ JR$_6$
								−0.049	$6\times$ JR$_{8f}$

[a] LOMO = NBO

last cage can be described [20] by either joint corazulenic flowers $12\times$[4:(7(5c)$_4$]JFw and simple rings $8\times$JR$_6$&$6\times$JR$_8$ or as joint corazenic co-Fws $8\times$[6:(5, 7)$_3$]co-JFw & $6\times$[8:(5, 7)$_4$]co-JFw & $12\times$R$_4$ (Fig. 8b).

Cage $240C/O-30$ (Fig. 8a) was designed by the $Tr_s(Ca_{3,2,C}(Me(M)))$ sequence, where $Ca_{(3,2)C}$ represents the pro-chiral generalized operation [21,22] $Ca_{(3,2)}$ with the faces of original map cut-off while Tr_s is the selected vertex truncation. This is the only operation sequence that put together two corazulenic patterns, being in a mutual relation by SW. The multiplication factor is $m = 5d_0$ in the triangulated Platonic or $m = 15$ in the trivalent dual pair, when no medial operation is added. Clearly, the two operation sequences: $Tr_s(Ca_{(3,2)C}(M))$ and $Le(P_5(M))$ are related by the SW edge-rotation.

Data for cages designed by $Le(P_5(M))/Le(P_5(Me(M)))$ operation sequences are given in Table 1. It can be seen that all the members of this family show deep

$60T$-15= $Le(P_5(G))$ Archimedean 4×[6:(5,6)$_3$]JFw & 4×JR$_6$ K :(3(0,3)^3) & (3)	$60T$-15= $Le(P_5(G))$ Archimedean 4×[6:(5,6)$_3$]co-JFw & 4×JR$_6$ K :(3(0,3)^3) & (3)
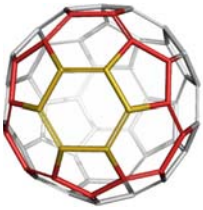	

Fig. 9 Sumanenic patterns in a tetrahedral, Archimedean covering of C_{60}

(a) 120C/O-15= $Le(P_5(G))$ or 120T-30= $Le(P_5(Me(G)))$ Archimedean 8×[6:(5,6)$_3$]JFw & 6×R$_8$ K :(3(0,3)^3) & (4) Archimedean 6×[8:(5,6)$_4$]co-JFw & 8×R$_6$ K :(4(0,3)^4) & (3)	**(b)** 120C-15= $Le(P_5(G))$ Platonic 24×DR$_5$ K :(0); [5]radialene
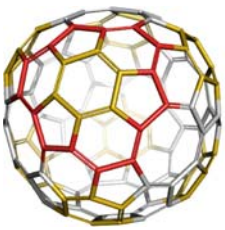	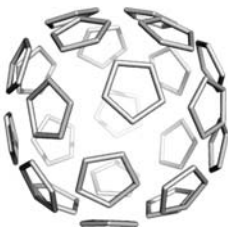

Fig. 10 Sumanenic covering

HOMO-LUMO gap, which is a characteristic of a closed π-electron shell as well as for Leapfrog fullerenes [23,24]. Note the non-bonding orbital NBO character of the LUMO orbital of cages containing octagons (Table 1, rows 2 and 3).

The first member of family is $60T-15 = C_{60}$. It is covered by four joint sumanenic flowers, in a tetrahedrally disposed Archimedean $4 \times [6:(5, 6)_3]$JFw & $4 \times JR_6$ covering (Fig. 9). Its π-electron local distribution, in terms of numerical Kekulé valence structure, is K:$(3(0, 3)^3)$ & (3) (see the top of figure). The above electronic distribution corresponds to the most important geometric Kekulé valence structure, as evaluated from the optimized inter-atomic distances by our JSCHEM software [25]. Data for $60T - 15$ (Table 1, first entry) are taken as reference for the stability of a fullerene. Its aromaticity (well theorized by Randic in a recent review [26]), show a rather low value of the well-known HOMA index [27] a result already reported [27,28].

The second member of this family is the cage $120C/O - 15$ or $120T - 30$ (Fig. 10 and Table 1, row 2). Its energetic data are close to $60T - 15$, but the overall aromaticity shows an anti-aromatic molecule (Table 1, row 2, column 7). Remarkably, this cage shows a 2-factor, also called a perfect Clar PC structure [23,29] consisting entirely of (empty, [5] radialenic) pentagons (24), in full analogy to $60T - 15$ (12 pentagons) and $240C/O - 30$ (48 pentagons). Together with the all-sumanenic main covering, this is a clear structural proof of the affiliation of these structures to the same structural

(a) 84*T*-21; [6:(5,6)$_3$]DFw Platonic	**(b)** 84*T*-21; [(6:6$_6$)&(6:(0,5)$_3$]co-JFw Archimedean
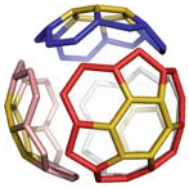	

Fig. 11 Platonic disjoint sumanenic covering $[n{:}(5,6))_{n/2}]$DFw,$n = s_{dd} = 6$ (**a**) and Archimedean joint coronenic and pentylenic $[(6{:}6_6)\&(n{:}(0,5))_{n/2}]co-JFw$, $n = s_{dd} = 6$; (**b**)

(a) 168*O*-21; [8:(5,6)$_4$]DFw Platonic	**(b)** 168*O*-21; [(6:6$_6$)&(8:(0,5)$_4$]co-JFw Archimedean
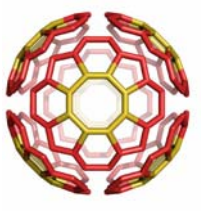	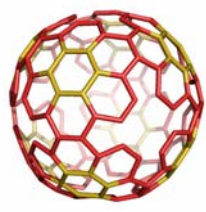

Fig. 12 Platonic disjoint sumanenic covering $[n{:}(5,6))_{n/2}]DFw$; $n = s_{dd} = 8$ (**a**) and Archimedean joint of coronenic $[n{:}6_n]Fw$, $n = s_{dp} = 6$ and pentylenic $[p{:}(0,5))_{p/2}]Fw$, $p = s_{dd} = 8$ tessellation (**b**)

family (the building operation sequence being mandatory in this respect). This is also supported by the energetic data: a value around 8 for the HF/Gap ratio, taken as a rough measure of molecular stability [30]. Strain energy, in terms of POAV1 theory [31–34] show decreasing values as the number of atoms increased. The value of 0.068 for HOMA index of $240C/O - 30$, predicts this, jet hypothetical molecule, as non-aromatic. Remark the co-existence of aromatic and anti-aromatic substructures in these cages, which are predicted rather stable by the energetic criteria.

4 Leapfrog related sequence

If the above section presented a joint sumanenic tessellation, the sequence $Le(S_2(T))$ (of non-commutative operations) provides a disjoint sumanenic $[n{:}(5,6)_{n/2}]$DFw; $n = s_{dd}$ pattern in a Platonic covering. The co-Fw forms an Archimedean joint of coronenic $[n{:}6_n]$Fw, $n = s_{dp}$ and pentylenic $[p{:}(0,5)_{p/2}]$Fw, $p = s_{dd}$ patterns [35]. The tripentylene [6:(0, 5)$_3$]Fw can be viewed as an analogue of the triphenylene [6:(0, 6)$_3$]Fw.

The size of the flowers' core is related to the size of faces of the parent p (Platonic cage), dual d or their double size; to specify the above relatedness the following symbols are used: s_p, s_d, s_{dp} and s_{dd}, respectively. Details of the covering are given in figures.

Table 2 Data for sumanenic $[n{:}(5,6)_{n/2}]$Fw; $n = s_{dd}$ cages (of $m = 21$) and their SW isomers: heat of formation per atom, HF (kcal/mol); HOMO-LUMO GAP (eV); HF/Gap($\times 100$; eV; PM3); strain energy per atom SE (kcal/mol; POAV1); total π-electron energy E_π (β-units; simple Hückel) and HOMA index of aromaticity

	Cage	Sym.	HF	Gap HF/Gap	SE	E_π shell	HOMA	HOMA-Fw	Fw
	1	**2**	**3**	**4**	**5**	**6**	**7**	**8**	**9**
1	$84T-21$	T	11.795	6.234	6.334	1.559	0.251	0.287	$4\times[6{:}(5,6)_3]$DFw
				8.213		cl		0.339	$4\times[(6{:}6_6)]$co-JFw
								0.139	$\&4\times[(6{:}(0,5)_3)]$co-JFw
2	$168O-21$	O	9.354	5.672	3.176	1.494	0.245	0.223	$6\times[8{:}(5,6)_4]$DFw
				7.158		cl		0.491	$8\times[(6{:}6_6)]$co-JFw
								−0.093	$\&6\times[(8{:}(0,5)_4)]$co-JFw
3	$168C-21$	O	17.312	6.477	4.456	1.556	−0.474	−0.009	$8\times[6{:}(5,6)_3]$DFw
				11.602		cl		−0.470	$6\times[(8{:}6_8)]$co-JFw
								0.165	$\&8\times[(6{:}(0,5)_3)]$co-JFw

The multiplication factor is $m = 7d_0$ in the triangulated Platonic or $m = 21$ in the trivalent dual pair. Figures 11 and 12 illustrate the above covering for the transforms of tetrahedron and octahedron, respectively. Table 2 gives the energetic data and aromaticity in terms of HOMA index.

These are quite stable structures, with the ratio HF/Gap lower than that of C_{60}. The most unstable appears the transform of cube $168C-21$ (Table 2, row 3, columns 3 and 4), which is anti-aromatic, according to the negative global HOMA value. Quite strange is tripentylene, the most aromatic substructure, in terms of HOMA, while [8] coronene $[(8{:}6_8)]$Fw is the most anti-aromatic, as expected. Note that $[n]$ circulenes with $n > 6$ have been synthesized [36,37].

E_π, calculated at Hückel level of theory (Table 2, column 6), does not fit neither with the PM3 data nor the HOMA results. The HOMO-LUMO gaps are well pronounced, as these cages show closed π-shells.

All the map operations have been performed by the CageVersatile CVNET software [38].

5 Conclusions

Sequences of classical or single generalized map operations were used to obtain $[n]$ circulenic flowers as covering patterns for nanostructures. Some Retro-operations, particularly the Retro–Leapfrog, have proved to be useful in investigating the tessellation of fullerenes, and on this ground, to formulate the affiliation of fullerenes, the C_{60} included, to a structural family.

This information was useful in understanding their closed π-electronic structure and related properties including the local aromaticity. The HOMA index enabled the evaluation of aromaticity of their various substructures.

Disjoint flower coverings are also designed by sequences of map operations. This could guide the future synthesis of fullerenes starting with flowers-templates to be next self-assembled in quasi-spherical cages.

Acknowledgement The paper is supported by the CEEX 41 Romanian GRANT, 2006.

References

1. T. Pisanski, M. Randić, Bridges between geometry and graph theory. In: *Geometry At Work: A Collection of Papers Showing Applications of Geometry* ed. by C.A. Gorini. Math. Assoc. Am. **53**, 174–194 (2000)
2. A.L. Mackay, H. Terrones, Nature **352**, 762–762 (1991)
3. Y-.D. Gao, W.C. Herndon, J. Am. Chem. Soc. **115**, 8459–8460 (1993)
4. P.W. Fowler, T. Heine, D.E. Manolopoulos, D. Mitchell, G. Orlandini, R. Schmidt, G. Seiferth, F. Zerbetto, J. Phys. Chem. **100**, 6984–6991 (1996)
5. M.V. Diudea, P.E. John, A. Graovac, M. Primorac, T. Pisanski, Croat. Chem. Acta **76**, 153–159 (2003)
6. M.V. Diudea, Studia Univ. "Babes-Bolyai" **48**(2), 3–16 (2003)
7. L. Euler, Comment. Acad. Sci. I. Petropolitanae **8**, 128–140 (1736)
8. L. Euler, Novi Comment. Acad. Sci. I. Petropolitanae **4**, 109–160 (1758)
9. F. Harary, *Graph Theory* (Addison-Wesley, Reading, MA, 1969)
10. M.V. Diudea, Forma (Tokyo) **19**, 131–163 (2004)
11. V. Eberhard, *Zur Morphologie der Polyeder* (Leipzig, Teubner, 1891)
12. P.W. Fowler, Chem. Phys. Lett. **131**, 444–450 (1986)
13. P.W. Fowler, J.I. Steer, J. Chem. Soc. Chem. Commun. 1403–1405 (1987)
14. J.R. Dias, MATCH, Commun. Math. Comput. Chem. **33**, 57–85 (1996)
15. M.V. Diudea, P.E. John, MATCH, Commun. Math. Comput. Chem. **44** , 103–116 (2001)
16. M.V. Diudea, P.E. John, A. Graovac, M. Primorac, T. Pisanski, Croat. Chem. Acta **76**, 153–159 (2003)
17. A.E. Vizitiu, M.V. Diudea, S. Nikolić, D. Janežić, J. Chem. Inf. Model. **46**, 2574–2578 (2006)
18. M.V. Diudea, A.E. Vizitiu, J. Math. Chem. (2008, this issue), doi:10.1007/s10910-008-9409-0
19. H. Sakurai, T. Daiko, T. Hirao, Science **301**, 1878 (2003)
20. H. Sakurai, T. Daiko, H. Sakane, T. Amaya, T. Hirao, J. Am. Chem. Soc. **127**, 11580–11581 (2005)
21. M.V. Diudea, M. Ştefu, P.E. John, A. Graovac, Croat. Chem. Acta **79**, 355–362 (2006)
22. M. Ştefu, M.V. Diudea, P.E. John, Studia Univ. "Babes-Bolyai", **50**(2), 165–174 (2005)
23. P.W. Fowler, T. Pisanski, J. Chem. Soc. Faraday Trans. **90**, 2865–2871 (1994)
24. P.W. Fowler, D.E. Manolopolous, *An Atlas of Fullerenes* (Oxford University Press, London, 1994), pp. 254–255
25. Cs.L. Nagy, M.V. Diudea, *JSCHEM Software Package* ("Babes-Bolyai" University, Cluj, 2005)
26. M. Randić, Chem. Rev. **103**, 3449–3605 (2003)
27. T.M. Krygowski, A. Ciesielski, J. Chem. Inf. Comput. Sci. **35**, 1001–1003 (1995)
28. P.W. Fowler, D.J. Collins, S.J. Austin, J. Chem. Soc. Perkin Trans. **2**, 275–277 (1993)
29. M.V. Diudea, in *Nanostructures-Novel Architecture*, ed. by M.V. Diudea (NOVA, New York, 2005), pp. 203–242
30. M.V. Diudea, Phys. Chem., Chem. Phys. **7**, 3626–3633 (2005)
31. R.C. Haddon, J. Am. Chem. Soc. **109**, 1676–1685 (1987)
32. R.C. Haddon, J. Am. Chem. Soc. **112**, 3385–3389 (1990)
33. R.C. Haddon, J. Am. Chem. Soc. **119**, 1797–1798 (1997)
34. R.C. Haddon, J. Am. Chem. Soc. **120**, 10494–10496 (1998)
35. M.V. Diudea, Cs.L. Nagy, in *Periodic Nanostructures*, Chap. 6 (Springer, 2007)
36. K. Yamamoto, Pure & Appl. Chern. **65**, 157–163 (1993)
37. M. Sato, K. Yamamoto, H. Sonobe, K. Yano, H. Matsubara, H. Fujita, T. Sugimoto, K. Yamamoto, J. Chem. Soc., Perkin Trans. **2**, 1909–1913 (1998)
38. M. Stefu, M.V. Diudea, CageVersatile CVNET Software (Babes-Bolyai University, 2005)